Influence of Subsurface Oxidation on the Structure, Stability, and Reactivity of Grafted Si(111) Surfaces

ARTICLE *in* THE JOURNAL OF PHYSICAL CHEMISTRY C · SEPTEMBER 2008

Impact Factor: 4.77 · DOI: 10.1021/jp711307p

4 AUTHORS, INCLUDING:

Fernanda Juarez
Universität Ulm
19 PUBLICATIONS **60** CITATIONS
SEE PROFILE

Federico Soria
National University of Cordoba, Argentina
7 PUBLICATIONS **28** CITATIONS
SEE PROFILE

Patricia Paredes-Olivera
National Scientific and Technical Research…
37 PUBLICATIONS **630** CITATIONS
SEE PROFILE

Influence of Subsurface Oxidation on the Structure, Stability, and Reactivity of Grafted Si(111) Surfaces

M. F. Juarez,[†] F. A. Soria,[‡] E. M. Patrito,[‡] and P. Paredes-Olivera*[,†]

Unidad de Matemática y Física and Departamento de Fisicoquímica, Instituto de Investigaciones en Fisicoquímica de Córdoba (INFIQC), Facultad de Ciencias Químicas, Universidad Nacional de Córdoba, Ciudad Universitaria, 5000 Córdoba, Argentina

Received: November 29, 2007; Revised Manuscript Received: June 19, 2008

We investigated the influence of intermolecular interactions and subsurface oxidation on the structure, surface bonding, and reactivity of compact monolayers of small organic and inorganic molecules bound to the Si(111) surface via Si−C, Si−N, and Si−O bonds. We considered the following modified surfaces: Si−CH_3, Si−CCH, Si−CN, Si−CH_2CH_3, Si−OCH_3, Si−OH, Si−NH_2, Si−NHOH, and Si−ONH_2. The highest hydrogen bond strength (7.5 kcal/mol) was observed for the (1 × 1) Si−NHOH monolayer. The (1 × 1) Si−CH_2CH_3 monolayer had the highest repulsion at the DFT level, 9.1 kcal/mol. However, inclusion of dispersion interactions yielded a repulsion of only 1.8 kcal/mol. Subsurface oxidation was investigated for −H, −CH_3, and −CH_2CH_3 terminated surfaces with surface coverages of 100 and 50%. The oxidation of the third Si−Si backbond is considerably more exothermic than the oxidation of the first and second backbonds. For monolayers with a surface coverage of 50%, the oxidation of alkylated silicon atoms is more stable than the oxidation of hydrogenated silicon atoms. The oxidation of alkylated silicon atoms stabilizes the organic monolayer for two reasons: a decrease of repulsive interactions between adjacent alkyl chains (due to the increase in intermolecular separations) and a strengthening of the Si−C surface bond. The reactivity of the grafted surfaces was investigated in the low coverage limit for the surface hydroxylation reaction with water. The highest activation barriers are obtained for the −CH_3 (40.3 kcal/mol) and −CH_2CH_3 (40.4 kcal/mol) terminated surfaces. The presence of conjugation in the organic molecule lowers the activation barrier. On the −CCH terminated surface, the activation energy decreases to 29.2 kcal/mol. The nucleophilic attack of silicon by water is facilitated on the −Cl, −OCH_3, and −NH_2 terminated surfaces due to the increased positive charge of the silicon atom. The −NH_2 and −Cl grafted surfaces are the most reactive with activation energies of 7.9 and 13.4 kcal/mol.

Introduction

Silicon is clearly the most technologically important material utilized today owing to its ubiquitous role in microelectronic computing. In spite of several decades of intense research into the properties and potential applications of silicon, the surface chemistry of this material has only recently begun to be investigated in a systematic fashion.[1] As electronic devices on silicon become progressively smaller, the fraction of atoms residing on or near the surface becomes significant. The chemical nature of these interface atoms thus plays a crucial role in the proper functioning and characteristics of the device. While native oxide on silicon has proven extremely useful in electronically passivating bulk silicon, much attention is being directed toward the synthesis of organic monolayers, which can be modified upon demand for specific requirements. Covalent attachment of organics to Si has attracted much attention, due to the ability to passivate the Si surface toward chemical oxidation while retaining desirable electrical properties.[2]

Silicon substrates offer several advantages compared to other surfaces:[3] (1) crystalline silicon is a well-defined surface; (2) ease and control of the preparation of atomically flat hydrogen-terminated silicon surfaces; (3) compatibility of the Si−H bonds terminating the surface with the main organic and organometallic reactions and a wide variety of organic functional groups; (4) formation of highly stable organic monolayers covalently bonded to the silicon surface through Si−C bonds; (5) use of the well-established micro- and nanofabrication methods for the integration of chemical and biochemical functionality into microelectronic platforms, and (6) intrinsic properties of silicon to detect molecular events occurring on the surface. However, there are some limitations to overcome before reaching stable and reusable devices based on organic monolayer/silicon hybrids and using the electronic properties of silicon for electrical detection of biomolecular events on the surface. The main drawback is the number of atop silicon atoms remaining unsubstituted after the chemical process. Because of the steric hindrance on the surface, the maximum surface coverage reachable is 50%[4−6] for long aliphatic alkyl chains with some early suggestions that the remaining silicon atoms are terminated with −OH[7] groups, with −H groups,[8,9] or with unidentified bonding states. The unsubstituted silicon atoms are not completely preserved against oxidation, which introduces electronic active surface defects on the surface. In a recent XPS study,[6] it was unambiguously established that a Si−C and Si−O−C linkage is formed after reaction with alkenes and decanol, respectively, and that the ungrafted sites remain H-terminated.

On the Si(111) surface, each silicon atop atom has only one Si−H bond, which is normal to the surface. Thus in principle, alkylation with small groups such as methyl can yield one alkyl group per Si surface atom. A fully methylated and atomically

* To whom correspondence should be addressed. E-mail: patricia@fcq.unc.edu.ar. Phone: 54-351-4344972.
[†] Unidad de Matemática y Física.
[‡] Departamento de Fisicoquímica.

10.1021/jp711307p CCC: $40.75
Published on Web 08/30/2008

flat Si(111) surface was obtained by anodization in a Grignard reagent.[10] Complete coverage of Si atop sites by CH_3 was also obtained through a two-step chlorination/Grignard process.[11] Methyl termination does not readily facilitate elaboration of the passivated $CH_3-Si(111)$ surface through subsequent chemical reactions. The covalent attachment of acetylene to every atop atom of the Si(111) surface has provided a scaffold for organic surface functionalization while retaining the Si−C passivation of Si(111) surface sites.[12,13]

When silicon is grafted with long alkyl chains, steric crowding limits the number of surface atoms that can be modified.[14] Quantitative surface coverages very close to the theoretical limit of 0.5 have been obtained on H−Si(111) from XPS[6] for alkyl and alkoxy monolayers and from IR[15] for carboxyl-terminated alkyl monolayers. Alkyl monolayers with a surface coverage higher than 0.42 provide long-term passivation of Si(111) against oxidation in air and water.[16] This threshold value corresponds to a monolayer with intermolecular channels narrower than the diameter of a water molecule which is thus excluded from penetrating into the monolayer and from oxidizing the unsubstituted Si−H groups of the surface.

On the H-terminated Si(111) surface, oxidation requires the presence of both an oxidant, O_2(g), and a nucleophile, H_2O.[17] Furthermore, the mechanism of oxidation of hydrogenated surfaces has been proposed to involve insertion of O into the Si−Si backbonds.[18−22] H−Si(100) surfaces are also oxidized in back-bond by several hundred hours exposure to humid air.[21,23]

The oxidation in air of alkylated Si(111) surfaces has been reported recently.[24] A detailed soft XPS study comparing the oxides on H-, CH_3-, and CH_2CH_3-terminated Si(111) surfaces has revealed that only Si suboxides are formed on alkylated surfaces, whereas SiO_2 forms as a result of the oxidation of H−Si(111) in ambient air. These observations suggest that replacement of surface Si−H or Si−Cl bonds by Si−C bonds fundamentally disrupts the mechanism of Si surface oxidation, not simply blocks the surface physically from ambient reactants.[24]

Periodic quantum mechanical calculations were performed to investigate the structure, packing, and strain energies of Si(111) grafted with $-CH_3$,[25,26] $-C_2H_5$,[26] $-C_6H_{13}$,[26] $-C_8H_{17}$,[26] and $-OCH_3$.[27] As expected, strain energies increase with molecular size and surface coverage, having an abrupt increase at a surface coverage of 0.75.[26] The thermodynamically controlled coverage of alkyl monolayers formed by the reaction of Cl-terminated Si surfaces with Grignard reagents was investigated for both linear as well as bulky alkyl groups.[26] The effect of oxygen incorporation on the Si−H vibrational frequencies of H−Si(100)-2 × 1 was investigated theoretically at the B3LYP level using cluster models of the oxidized surface.[28]

The structure and stability of organic layers on solid surfaces depend on the interactions with the surrounding molecules[29,30] and on surface bonding. The knowledge of these factors is necessary to understand the thermal stability of the organic monolayer. In this work, we undertook a comprehensive investigation of the stability of high coverage structures of small organic and inorganic molecules bound to the Si(111) surface via Si−C, Si−N, and Si−O bonds. The effect of intralayer hydrogen bonding interactions on the structure and stability of OH- and NH_2-terminated monolayers was investigated. It has been reported experimentally that subsurface oxidation produces an important shift in the Si−H vibrational frequency.[18,28] However, the influence of subsurface oxidation on the energetics, structure, and stability of compact monolayers has not been investigated yet. These issues were investigated in the present work for methyl and ethyl monolayers with surface coverages of 50 and 100%.

The strength of the surface bonding is not necessarily related to the reactivity of the grafted surface toward a given reactant. The activation energy barrier of the transition structure is the relevant parameter to determine the surface reactivity. We therefore used the hydroxylation reaction with water as a model reaction to investigate the reactivity of the different grafted surfaces.

Theoretical Methods and Surface Modeling

The (111) face of silicon was modeled by means of a silicon slab six layers thick. Periodic boundary conditions were applied to avoid edge effects. The dangling bonds of the bottom surface were saturated with hydrogen atoms. The silicon atoms of the lower bilayer were kept fixed in a bulk-terminated configuration. The positions of all the adsorbate atoms as well as those of the four topmost Si layers were fully optimized. The unit cells employed were (1 × 1) and (2 × 2). A vacuum thickness of 10 Å was introduced between the slabs to avoid spurious interactions between neighboring replicas. The first principle atomistic calculations were performed using state of the art plane wave periodic DFT as implemented in the PWSCF code.[31] Ultrasoft pseudopotentials[32] were used for the atomic species. Gradient corrections were included in the exchange correlation functional using the PBE formulation.[33] The electron wave functions were expanded in a plane-wave basis set up to a kinetic energy cutoff of 26 Ry (200 Ry for the density). Brillouin zone integration was performed using a (4 × 4 × 1) Monkorst-Pack mesh.[34]

Local Møller−Plesset second-order perturbation theory (LMP2)[35−38] calculations were performed to evaluate intermolecular interactions in molecular clusters of methane, ethane, methanol and acetylene with an intermolecular separation of 3.84 Å. In LMP2, unlike in canonical MP2, the correlating virtual space for each occupied orbital is limited to those orbitals that are localized on the atoms of the local occupied Hartree−Fock (HF) orbital. The Pipek−Mezey[39] localization procedure was used. For the computation of intermolecular interactions, local electron correlation methods[37,38] have proven to be particularly useful, as by construction they are virtually free of basis set superposition errors (BSSE)[37] provided the BSSE is small at the HF level. This makes it possible to perform geometry optimizations for larger clusters without counterpoise corrections. We employed the correlation consistent basis sets of Dunning et al.[40] as the AO basis set. Geometry optimizations were performed with the cc-pVTZ basis sets (without f orbitals), and the energy calculations were performed with the cc-pVQZ basis sets (without g orbitals). LMP2 geometry optimizations and single point energy evaluations were done with the Jaguar suite of programs.[41]

The reactivity of the grafted surfaces toward water was investigated in the low coverage limit using cluster models of the surface. The cluster was terminated by hydrogen atoms to satisfy the valency of the cleaved Si−Si bonds during excision from the extended surface. The hydrogenated Si(111) surface was modeled with a $Si_{22}H_{28}$ cluster whereas the oxidized surface was modeled with a $Si_{40}O_3H_{64}$ cluster. These calculations were carried out using the Jaguar suite of programs[41] at the PBE/6-31G** level of theory. We therefore used the same functional in the periodic as well as in the cluster calculations. Minimum energy structures were calculated for the reactants and transition structures. The nature of the calculated structures was verified by subsequent harmonic frequency calculations.

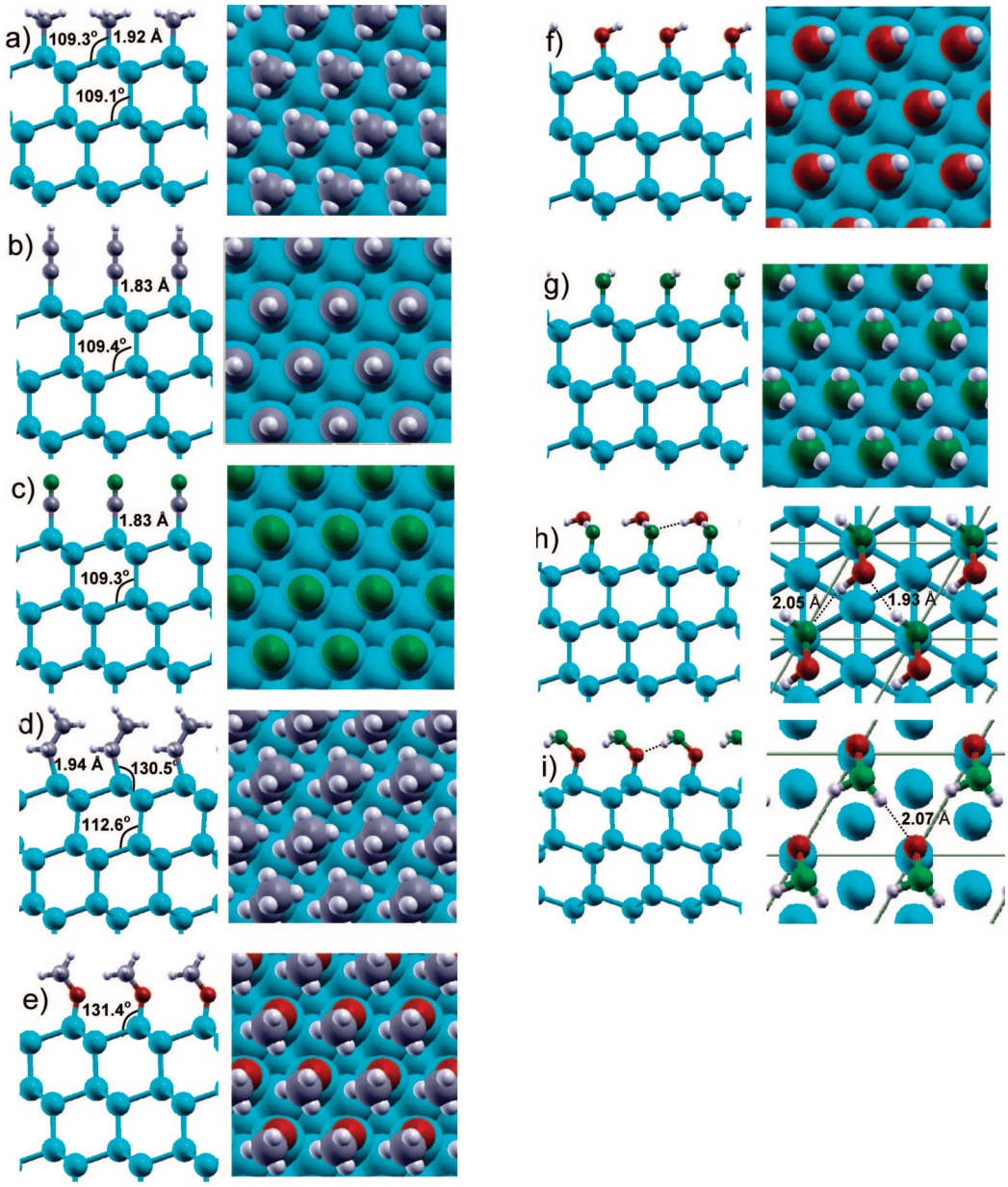

Figure 1. Side and top views of the equilibrium structures with a 100% surface coverage. Calculations performed with a 1 × 1 unit cell. (a) $-CH_3$, (b) $-CCH$, (c) $-CN$, (d) $-CH_2CH_3$, (e) $-OCH_3$, (f) $-OH$, (g) $-NH_2$, (h) $-NHOH$, (i) $-ONH_2$.

Results and Discussion

Structure and Stability. The formation of CH_3 and CCH monolayers with a surface coverage of 100% has been reported experimentally by the two-step chlorination/alkylation method.[12,13] Although the free energy change for the formation of an ethyl monolayer at full coverage is negative for the reaction involving Grignard reagents,[14] the highest surface coverage observed experimentally was 77%.[20] In the case of CH_3O monolayers, the maximum coverage observed was around 50%,[42] although the formation of a compact monolayer is feasible from a thermodynamic point of view.[43]

Figure 1 shows the equilibrium structures at high coverage for all the monolayers investigated. The same structures were obtained using 1 × 1 and 2 × 2 unit cells. In the case of a bare CH_3 monolayer (with the same C−C separation as on the Si(111) surface at full coverage), the energy landscape as a function of the rotation angle of the methyl moiety (Figure 2a) closely follows the interatomic distance between the adjacent hydrogen atoms (Figure 2b). The equilibrium energy is obtained at an angle of 30°, which corresponds to a structure with the same separation for all hydrogen atoms (Figure 2b). The effect of the surface on the potential energy landscape is shown in Figure 2c for a coverage of 25%. For this coverage, the minimum energy is observed for a SiSiCH dihedral angle of 60%. For this configuration, the distance between the H atom of the CH_3 group and the nearest silicon atom of the second layer is maximum (distance d3, Figure 2d) whereas the H atom of CH_3 is equidistant from the H atoms of the adjacent SiH groups (d1 = d2 at 60°). The relative minimum at 35° corresponds to a configuration in which the H atom of CH_3 is equidistant from the Si atom of the second layer and the nearest H atom of the adjacent SiH group.

Figure 3 shows the influence of the surface coverage on the potential energy profiles as a function of the rotation angle. The different local minima reflect the predomination of adsorbate−substrate interactions or adsorbate−adsorbate interactions. As the repulsion between adjacent H atoms of the $-CH_3$ groups becomes predominant, the equilibrium SiSiCH dihedral angle changes

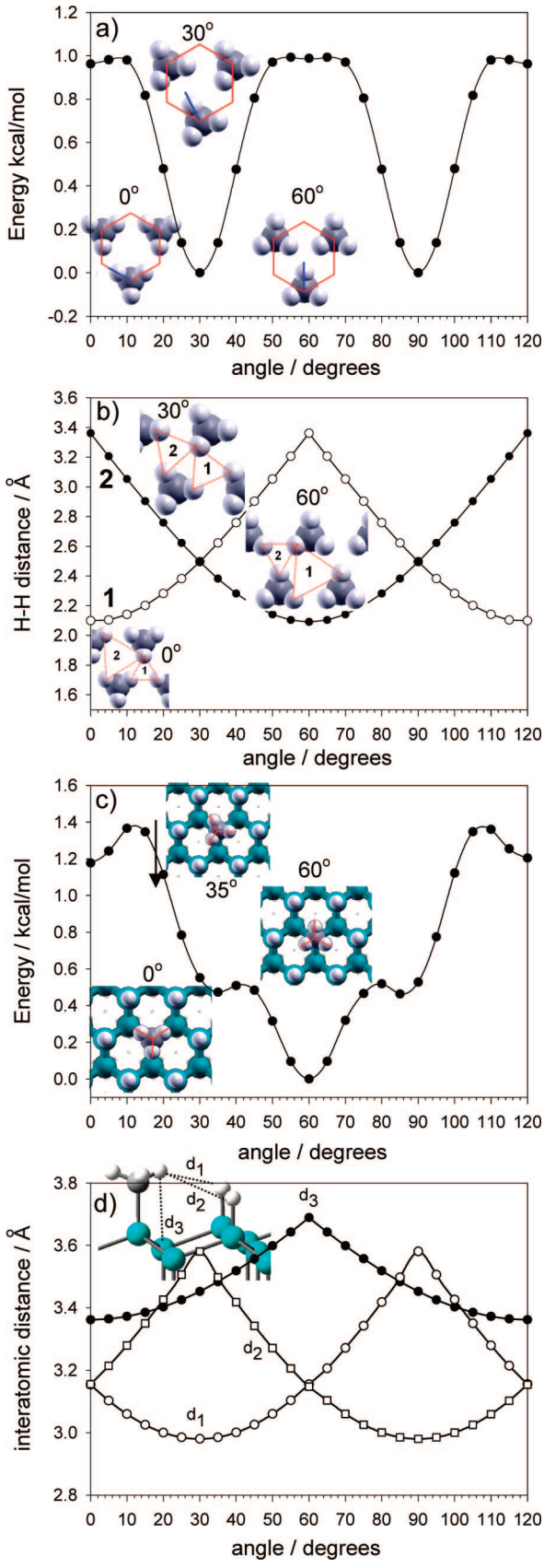

Figure 2. (a) Potential energy and (b) H−H distance for a monolayer of bare CH_3 groups with the same geometry as on the Si(111) surface with 100% surface coverage. The red hexagon of the insets indicates the position of the silicon atoms of the first bilayer when the CH_3 group is adsorbed on the surface. (c) Potential energy and (d) interatomic distances as a function of the SiSiCH dihedral angle for a monolayer with a 25% surface coverage (2 × 2 unit cell).

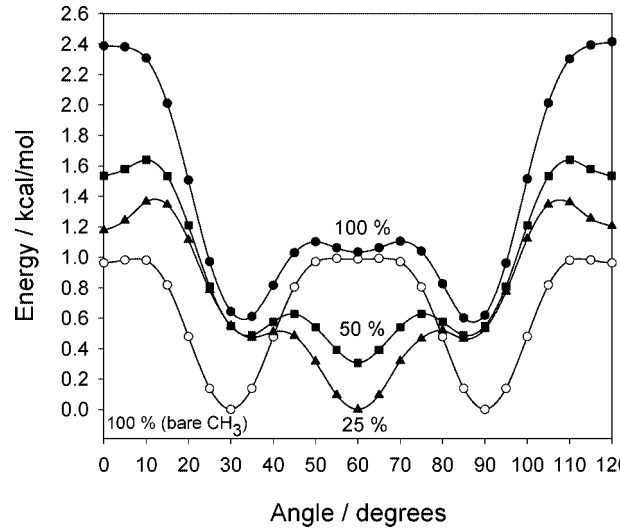

Figure 3. Potential energy as a function of the SiSiCH dihedral angle for CH_3 surface coverages of 25 (▲), 50 (■), and 100% (•). The open circles correspond to a bare monolayer with the same structure as on the Si(111) surface with 100% surface coverage.

from 60 to 37.8° at full coverage. This value contrasts with the experimental value of 23 ± 3° obtained from STM.[11] However, DFT calculations showed that the chlorination-methylation of the hydrogen terminated Si(111) surface can induce a stacking fault in the presence of etch pits which explains the experimental angle of 23 ± 3°.[25]

The CH_3, CCH, and CN terminated monolayers induce a minor relaxation of the silicon lattice, with SiSiSi angles of 109.1 (Figure 1a), 109.4 (Figure 1b), and 109.3° (Figure 1c), respectively, which are very close to the tetrahedral angle of 109.5°. On the contrary, the SiSiSi and SiCC angles for the ethyl monolayer (Figure 1d) show that this monolayer is strained at full coverage. The SiSiSi angle of 112.6° for the ethyl monolayer is larger than the nearly tetrahedral value of 109.1° observed for the methyl monolayer. The SiCC angle is 130.5° at full coverage (Figure 1d); however, at a coverage of 25% it decreases to 117.6°. The value of the SiCC angle at full coverage compares very well with a previous calculation in which an angle of 130.8° was obtained.[44] The same trend is observed for the methoxi monolayer. The SiOC angle increases from 129.7° (25% coverage) to 131.4° at full coverage (Figure 1e).

The hybridization of the carbon atom bound to the silicon surface influences the Si−C bond length as well as the bond strength as it will be shown below. The CCH and CN monolayers bound to the surface via a carbon atom with an sp hybridization have the shortest Si−C bond lengths (1.83 Å, Figure 1b,c) whereas the methyl and ethyl monolayers have Si−C bond lengths of 1.92 (Figure 1a) and 1.94 Å (Figure 1d), respectively.

The distances between a hydrogen atom and the nearest neighbor O or N atom in the OH and NH_2 monolayers are 3.20 (Figure 1f) and 3.15 Å (Figure 1g), respectively. These large distances indicate that the formation of a strong hydrogen bond is not possible. However, in the case of monolayers formed from hydroxylamine, either the Si−N (Figure 1h) or the Si−O (Figure 1i) surface bonding configurations produce monolayers that are stabilized by hydrogen bonding. In the case of the Si−NHOH monolayer (Figure 1h), the OH···N hydrogen bond length is 2.05 Å and the NH···O HB length is 1.93 Å; for the Si−ONH_2 monolayer (Figure 1i), the NH··O hydrogen bond length is 2.07 Å.

TABLE 1: Energy Change for the Reaction Si(111) − R → Si(111)· + R· Calculated for Surface Coverages of 100 and 25%; energies in kcal/mol

R	ΔE^{100}	ΔE^{25}	$\Delta E^{25} - \Delta E^{100}$
$-CH_3$	80.0	82.0	2.0
$-CH_2CH_3$	66.0	75.1	9.1
−CN	100.2	105.6	5.5
−CCH	110.6	113.2	2.6
$-OCH_3$	87.9	88.9	1.0
−OH	109.2	107.8	−1.4
$-ONH_2$	80.3	77.3	−3.0
−NHOH	77.9	70.5	−7.5
$-NH_2$	84.8	86.5	1.7
−Cl	96.9	99.3	2.4
−H	78.4	78.8	0.4

Binding energies were calculated from the energy change of the reaction

$$\text{Si(111)}-\text{R} \rightarrow \text{Si(111)}\cdot + \text{R}\cdot \quad (1)$$

There are two contributions to the magnitude of binding energies: the strength of the surface chemical bond and intermolecular interactions. Binding energies are reported in Table 1 for surface coverages of 100 and 25%. In the case of monolayers bound via a C atom, the binding energies are more than 20 kcal/mol stronger for sp hybridization (CCH and CN) than for sp^3 hybridization (CH_3 and CH_2CH_3). Table 1 shows that the highest binding energies are observed for the −CCH, −OH, and −Cl groups.

Intermolecular Interactions. Intermolecular interactions are reflected in Table 1 in the binding energy differences at both coverages. The interactions calculated at the DFT level are repulsive (positive values) for most monolayers except for those in which hydrogen bonding occurs. At full coverage, the highest repulsive interactions are observed for the bulkiest groups, $-CH_2CH_3$ and −CN. In the case of the −OH, $-ONH_2$, and −NHOH monolayers, the full coverage structure is more stable than the 25% coverage by 1.4, 3.0, and 7.5 kcal/mol, respectively. In the last two cases, the stabilization is due to hydrogen bonding as discussed in the previous section. In the case of the −OH terminated surface, the small stabilization probably arises from the alignment of surface dipoles. For the rest of the groups, the interactions are repulsive with values ranging from 0.96 to 2.6 kcal/mol.

As DFT does not take into account dispersion interactions, we performed LMP2 calculations using molecular clusters as shown in Figure 4. The clusters were optimized at the LMP2 level with different constraints to simulate adsorption on a Si(111) surface. The bottom hydrogen atoms were kept fixed on the same plane with a separation of 3.84 Å, which corresponds the interatomic distance of bulk silicon. The interatomic distances of the other C or O atoms were also kept fixed at 3.84 Å. The angle between the plane containing the bottom hydrogen atoms and the HC and HO bonds was kept fixed with the same value as the angle between the silicon surface and the Si−C or Si−O bonds. The interaction of the central molecule in the cluster with the surrounding six molecules was calculated from the corresponding energy differences. Table 2 compares the interaction energies at the LMP2 level with the value obtained from DFT on the silicon surface. For the methane cluster, an attractive interaction of −0.72 kcal/mol is observed, whereas for the other molecules a small repulsion exists at the intermolecular distance of 3.84 Å. As expected, the repulsion is lower at the LMP2 level as it accounts for attractive dispersion interactions. The major difference is observed for the ethane molecule, for which the repulsion at the LMP2 level is much lower than that at the DFT level. The LMP2 result shows that the repulsion is low even though the interatomic distance of 3.84 Å is much smaller than the typical van der Waals diameter of 5.4−5.0 Å of alkyl chains.[45] This explains why high ethyl coverages around 80% have been reported with different experimental techniques.[8,24]

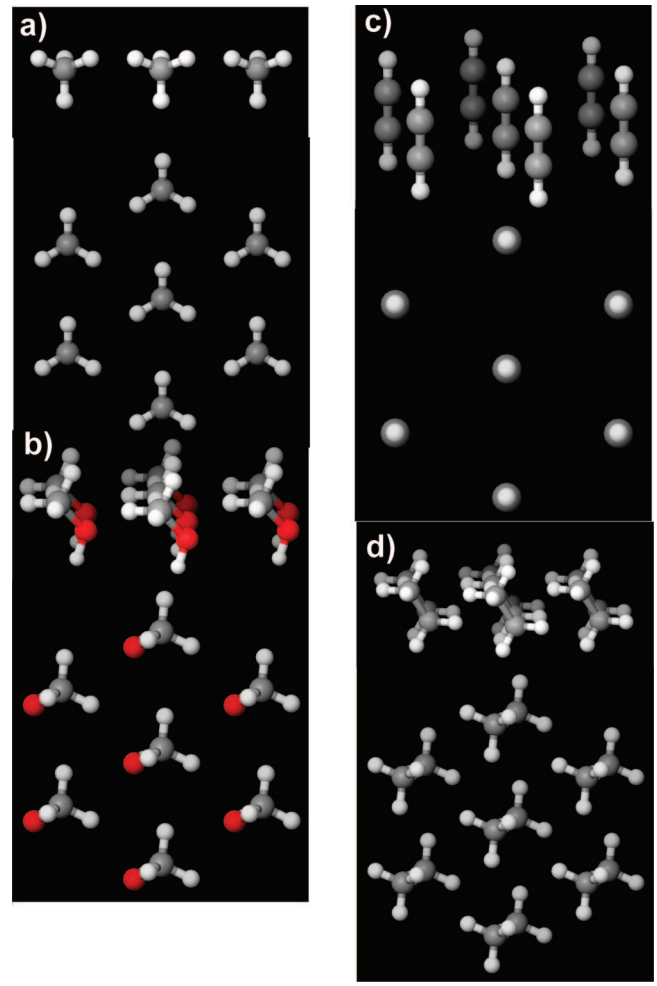

Figure 4. Side and top views of clusters with an intermolecular separation of 3.84 Å. (a) CH_4, (b) CH_3OH, (c) HCCH, and (d) CH_3CH_3.

TABLE 2: Molecular Interactions Calculated at a Separation of 3.84 Å with the Same Geometry As on the Si(111) Surface at Full Coverage[a]

molecule	LMP2	DFT
$H-CH_3$	−0.72	1.95
$H-OCH_3$	0.18	0.96
H−CCH	1.22	2.61
$H-CH_3CH_3$	1.76	9.13

[a] In the LMP2 calculation a molecular cluster is used. In the DFT calculation a molecular slab is used. Energies in kcal/mol.

Energetics of Surface Reactions. The energy changes involved in the formation of the monolayers from the corresponding RH molecules in the gas phase were evaluated for the hydrogenated and chlorinated surfaces according to the reactions

$$\text{Si(111)}-\text{H} + \text{RH}_{(\text{gas})} \rightarrow \text{Si(111)}-\text{R} + \text{H}_{2(\text{gas})} \quad (2)$$

$$\text{Si(111)}-\text{Cl} + \text{RH}_{(\text{gas})} \rightarrow \text{Si(111)}-\text{R} + \text{HCl}_{(\text{gas})} \quad (3)$$

The results are summarized in Table 3. Reaction 2 is endothermic for methane and ethane but becomes exothermic

TABLE 3: Energy Changes for the Reaction of RH with the Hydrogenated and Chlorinated Surfaces: Si(111)−H + RH → Si(111)−R + H_2 and Si(111)−Cl + RH → Si(111)−R + HCl, respectively; energies in kcal/mol

RH	Si(111)−H	Si(111)−Cl
CH_4	8.90	22.0
C_2H_6	19.4	32.5
HCCH	−0.75	12.4
HCN	1.5	14.7
NH_3	0.32	13.5
NH_2OH	−7.5	5.7
ClH	−13.1	0.0
H_2O	−10.3	2.8
H_3COH	−8.4	4.7

for Si−N and Si−O linkages as well as for Si−C linkages involving a C atom with sp hybridization. The fact that the reaction with methanol is exothermic is in agreement with the experimental result showing that alkoxy monolayers are formed upon immersion in liquid methanol.[42] The reactions on the chlorinated surface are endothermic for all reactants. The ΔE values on the chlorinated surface are 13.1 kcal/mol higher than on the hydrogenated surface. This is mainly due to the fact that the Si−Cl bond energy is higher than the Si−H bond energy as shown in Table 1. These results suggest that the chlorinated surface should be less reactive than the hydrogenated surface, which is contrary to the experimental evidence that upon exposure to air, the Si(111)−Cl surface readily oxidizes.[24] The energetics of reactants and products is not enough to explain the experimental trend. The calculation of energy barriers is required for a complete understanding of the surface reactivity. This issue will be considered in detail elsewhere.[46] In the next section, we investigate the reactivity of the grafted surfaces with the water molecule by calculating the corresponding activation energy barriers.

Reactivity of Grafted Surfaces. The reactivity of the grafted surfaces was investigated for the surface hydroxylation reaction with the water molecule. Figure 5 shows the activation energy barriers and interatomic distances for the transition structures. In the transition complex, one of the OH bonds of water enlarges from the equilibrium value of 0.973 Å. On the S−H, Si−CH_3, Si−CH_2CH_3 and Si−CCH surfaces, the OH bond length of the activated complex is in the range 1.11−1.15 Å. The highest enlargement was obtained for the −NH_2 and −OCH_3 grafted surfaces (around 1.33 Å, Figure 5f,g), whereas in the case of the chlorinated surface (Figure 5h) the smallest elongation was calculated (0.998 Å). Si−O distances are in the range of 1.81−2.15 Å in the activated complexes whereas for the hydroxylated surface the equilibrium Si−OH bond length is 1.703 Å.

The methylated and ethylated surfaces have nearly the same activation barriers: 40.3 and 40.4 kcal/mol, respectively. These values are higher than on the hydrogenated surface (28.4 kcal/mol). This correlates with the increased passivating capacity of alkyl monolayers grafted on silicon.[24]

In the series of −CH_2CH_3, −$CHCH_2$, and −CCH grafted surfaces, the activation energy decreases monotonically: 40.4, 33.7, and 29.2 kcal/mol. Therefore, the introduction of conjugation in the organic molecule increases the reactivity toward water. We attribute the lowering of the activation energy barrier to the stabilization of the delocalized electron density of the transition state by the π systems of the −$CHCH_2$ and −CCH molecules. The role of molecular conjugation on the stabilization of transition states has been reported for other reactions on Si(111).[47]

The activation barrier for the hydroxylation of the −CCH grafted surface (29.2 kcal/mol) is considerably lower than that of the methylated surface (40.3 kcal/mol). This shows that the CCH monolayer is more reactive toward water even though the Si−C bond strength for this monolayer is ca. 30 kcal/mol higher than the Si−C bond of the methyl grafted surface (Table 1).

In the case of −NH_2, −OCH_3, and −Cl grafted surfaces (Figure 5f−h), much lower activation energy barriers are obtained: 7.9, 16.3, and 13.4 kcal/mol, respectively. The NBO[48] charges of the silicon atom in these transition structures are +0.71, +0.80, and +0.51 au, respectively, whereas the charge of the silicon atom is only +0.43 au in the transition structure of the hydrogenated surface (Figure 5a). This shows that the electronegative N, O, and Cl atoms increase the positive charge of the Si atom in the transition complex. This favors the nucleophilic attack of the water molecule with the corresponding reduction of the energy barrier.

The fact that the chlorinated surface readily oxidizes upon exposure to air[24] whereas the hydrogenated surface is much better passivated correlates with the magnitude of the corresponding energy barriers: 13.4 (Cl−Si(111)) and 28.4 kcal/mol (H−Si(111)). The stabilization of the transition complex for the chlorinated surface arises from the polarization of the water molecule produced by the positively charged silicon atom (+0.52 au) and the negatively charged chorine atom (−0.50 au).

This effect is also observed in the case of subsurface oxidation. Figure 5i and 5j show the transition structures for the hydroxylation of the O_3Si−H and O_3Si−CH_3 groups. The oxidized silicon atom has a charge of +2.19 (Figure 5i) which is larger than the charge of +0.43 of the unoxidized silicon atom in the transition structure of Figure 5a. This induces a decrease of the activation barrier for the Si−H hydroxylation from 28.4 kcal/mol (Figure 5a) to 22.7 kcal/mol for the oxidized surface (Figure 5i). The same trend is observed for the Si−CH_3 hydroxylation: the activation barrier decreases from 40.3 (Figure 5b) to 31.2 kcal/mol (Figure 5j).

Subsurface Oxidation of the Fully Methylated Surface. The equilibrium structures for the oxidation of one, two, and three Si−Si backbonds of a fully methylated surface are shown in Figure 6. In all cases the equilibrium geometry of the oxidized backbond has the oxygen atom on the upper side of the line connecting both silicon atoms as shown in the side views of Figure 6. The successive oxidation leads to an upward shift of the CH_3Si moiety. Si−Si bonds shorter than 2.30 Å have been connected by a line in the top views of Figure 6. It can be observed that Si atoms bonded to oxygen atoms have shorter bond lengths with the nearest neighbor Si atoms. The average Si−Si bond length of silicon atoms bonded to oxygen atoms is 2.30 Å whereas the average Si−Si bond length of the remaining silicon atoms is 2.37 Å. Oxidized silicon atoms also have shorter Si−C bond lengths than nonoxidized atoms as shown in Table 4, which compares the Si−C bond lengths for the 1 × 1 compact monolayers and the 2 × 2 structures with one silicon atom trioxidized (Figure 6c, for example). The shortening of the bond length implies a strengthening of the surface bond. The same effect is observed for the hydrogenated surface.

The methyl and hydrogen binding energies were calculated as a function of the degree of silicon oxidation. Figure 7 shows the change in binding energy as a function of the number of oxygen atoms in the backbonds for a methylated and a hydrogenated surface. The major increase in the binding energy is observed after the addition of the third oxygen atom. The methyl binding energy is 18.4 kcal/mol higher on a trioxidized silicon atom than on the nonoxidized surface, whereas the

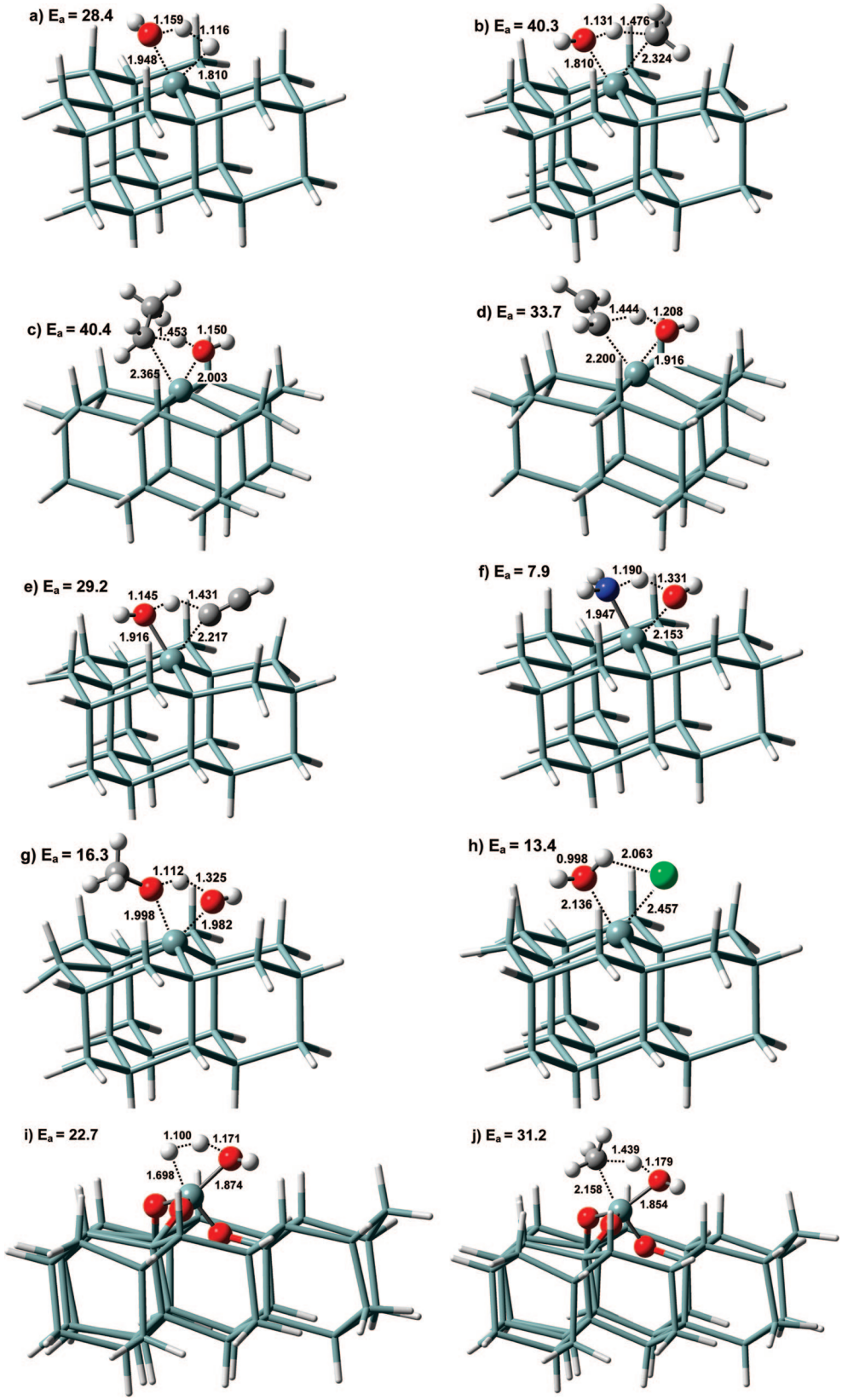

Figure 5. PBE/6-31G** optimized transition structures for the surface hydroxylation reaction between water and the following grafted surfaces: (a) Si−H, (b) Si−CH_3, (c) Si−CH_2CH_3, (d) Si−$CHCH_2$, (e) Si−CCH, (f) Si−NH_2, (g) Si−OCH_3, (h) Si−Cl, (i) O_3Si−H, and (j) O_3Si−CH_3. Activation energies are in kcal/mol and interatomic distances are in ångstroms. For the sake of clarity, the atoms involved in the transition structure are plotted with ball and sticks. The interatomic bonds of rest of the cluster are plotted as sticks. A Si_{22} cluster was used in calculations of panels a−h and a $Si_{40}O_3$ cluster was used in the calculations of panels i and j. The reference state for the calculation of the energy barrier is the water molecule in the gas phase and the corresponding grafted surface.

corresponding difference is lower on the hydrogenated surface: 13.9 kcal/mol.

These results correlate with thermal stability studies. On the unoxidized surface, the decomposition of alkyl monolayers

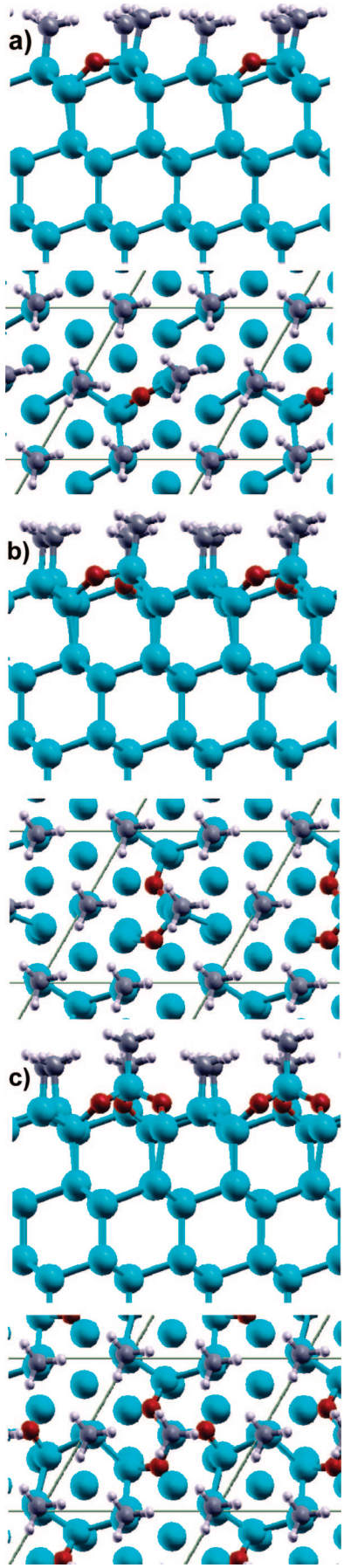

Figure 6. Silicon backbond oxidation of a fully methylated surface with (a) one, (b) two, and (c) three oxygen atoms. The side and top views correspond to the equilibrium structure calculated with a 2 × 2 unit cell.

TABLE 4: Si−R Bond Lengths on Unoxidized (Si_3Si-R) and Oxidized (O_3Si-R) Surfaces with 100% Surface Coverage of R[a]

R	Si_3Si-R	O_3Si-R
H	1.50	1.48
CH_3	1.92	1.86
CH_2CH_3	1.94	1.87
CCH	1.83	1.81

[a] The calculations were performed with a 2 × 2 unit cell. Bond lengths in ångstroms.

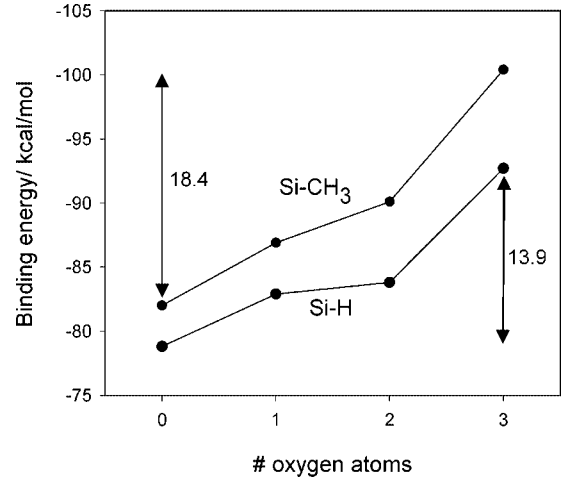

Figure 7. Binding energies of $-CH_3$ and $-H$ as a function of the number of oxygen atoms in the backbonds (see Figure 6).

TABLE 5: Energetics of the Surface Reactions with Water for the Successive Oxidation of Silicon Backbonds for Monolayers with a 100% Coverage of R[a]

	R		
	H	CH_3	CCH
$(Si_3)Si-R + H_2O \rightarrow (Si_2O)Si-R + H_2$	−2.9	−0.6	+3.5
$(Si_2O)Si-R + H_2O \rightarrow (SiO_2)Si-R + H_2$	−6.1	−8.1	−8.7
$(SiO_2)Si-R + H_2O \rightarrow (O_3)Si-R + H_2$	−15.0	−19.5	−20.3
total ΔE	−24.0	−28.2	−25.5

[a] Calculations performed with a 2 × 2 unit cell. Energies in kcal/mol.

produces alkenes via the Si−C bond cleave according to a β-hydride elimination.[49,50] However, on the oxidized silicon surface, the Si−C bonds remain intact and the decomposition of the monolayer initially occurs primarily through C−C bond cleavage.[51] Therefore, the strengthening of the Si−C bond by 18.4 kcal/mol due to subsurface oxidation explains its increased thermal stability.

The energy changes for the successive oxidation of the backbonds for the fully methylated and acetylated surfaces in comparison to the hydrogenated surface are shown in Table 5. The oxidation of the first backbond is slightly exothermic on the hydrogenated surface whereas on the acetylated surface is endothermic. The oxidation on the second and third backbonds is more exothermic on the grafted surfaces than on the hydrogenated surface. On all surfaces, the oxidation of the third backbond is considerably more exothermic than the oxidation of the first and second backbonds. This is consistent with the experimental observation showing that the oxide formed on alkylated silicon surfaces is predominantly Si(III) in character.[24]

Subsurface Oxidation of Methyl and Ethyl Monolayers with 50% Coverage. The influence of silicon oxidation on the stability of the alkyl monolayers was also investigated for

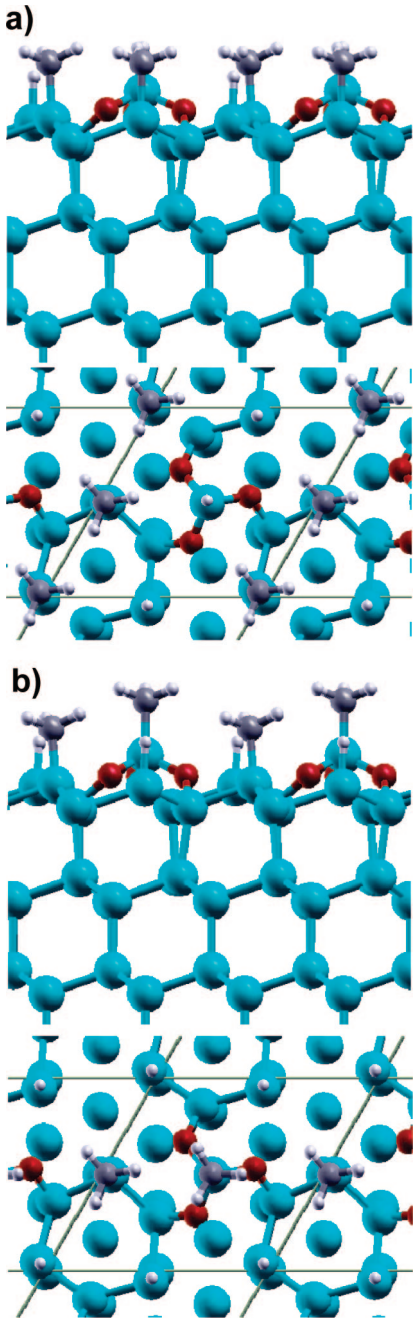

Figure 8. Oxidation of a silicon surface with a 50% coverage of methyl groups. Side and top views of the backbond oxidation of (a) the SiH moiety and (b) the $SiCH_3$ moiety.

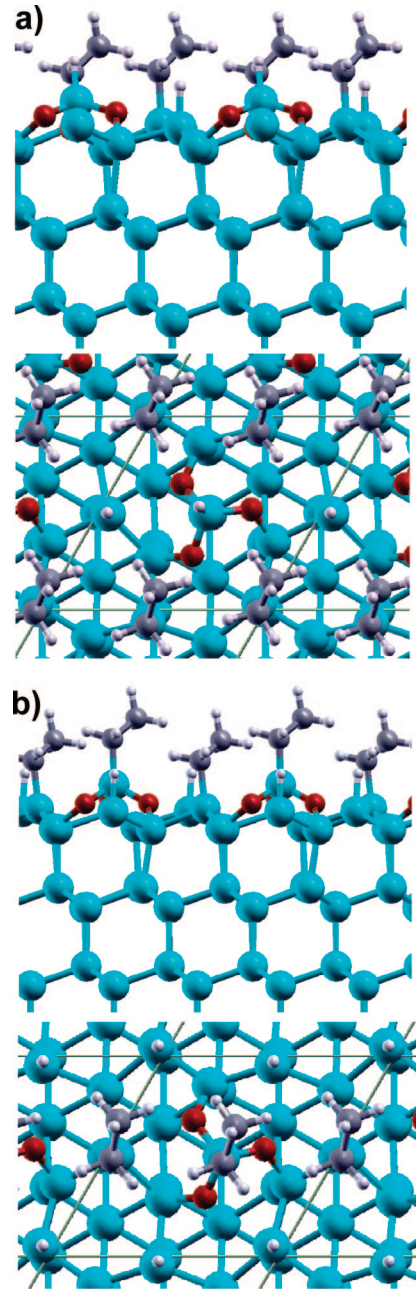

Figure 9. Oxidation of a silicon surface with a 50% coverage of ethyl groups. Side and top views of the backbond oxidation of (a) the SiH moiety and (b) the $SiCH_2CH_3$ moiety.

methylated and ethylated surfaces with a coverage of 50%. On each surface, we considered the oxidation of the Si−H, Si−CH_3, and Si−CH_2CH_3 groups. Figure 8 shows top and side views of the equilibrium geometries of the methylated surface. The oxidation of the hydrogenated silicon atom has a minor effect on the geometric parameters of the adjacent Si−CH_3 groups. However, the oxidation of the methylated silicon atom increases the interatomic distance between the hydrogen atoms of adjacent CH_3 groups from the value of 2.32 Å corresponding to the fully methylated surface (Figure 1a) to an average value of 2.50 Å.

In the case of the oxidized ethylated surface (Figure 9), the average hydrogen distance between adjacent CH_2CH_3 groups is 2.56 Å which is larger than the value of 2.29 Å corresponding to the unoxidized surface (Figure 1d). This increase in interatomic distances has a stabilizing effect as the interactions between adjacent molecules are repulsive. The subsurface oxidation also produces a shortening of the Si−C bond length which indicates a strenghening of this bond. On the methylated surface (Figure 8b) the Si−C bond length is 1.86 Å on the trioxidized Si atom whereas on the unoxidized Si atom this bond length is 1.91 Å (Figure 8a). The same effect is observed on the ethylated surface for which the corresponding bond lengths are 1.87 (Figure 9b) and 1.94 Å (Figure 9a), respectively.

In summary, the oxidation of alkylated silicon atoms stabilizes the organic monolayer for two reasons: a decrease of repulsive interactions between adjacent alkyl chains (due to the increase in intermolecular separations) and an increase in the Si−C surface bond strength. This is effectively observed in the energy difference between the structure in which the oxidized silicon atom is bound to an alkyl chain and the structure with the backbonds of the SiH group oxidized. The oxidation of the alkylated silicon atom always produces the most stable structure.

The structure with the oxidized methylated silicon atom (Figure 8b) is 5.4 kcal/mol more stable than the structure in which the hydrogenated silicon atom is oxidized (Figure 8a). The corresponding difference for the ethylated surface is more pronounced: the structure in Figure 9b is 10.4 kcal/mol more stable than the structure in Figure 9a. The higher stability of the structure in which the alkylated silicon atom is oxidized reveals the decrease of repulsive interactions due to the increase in the separation between the hydrogen atoms of adjacent chains, as discussed in the previous paragraph.

In order to further evaluate the effect of subsurface oxidation on the decrease of repulsive interactions between the organic chains, we repeated the calculations for a Si(111) surface with a 50% coverage of acetylene groups. The repulsion between acetylene groups is lower than between ethylene groups, from which we expect that the oxidation of grafted or ungrafted silicon atoms should produce structures with similar energies. This is effectively observed. The oxidation of the silicon atom bound to the CCH group produced a structure which is more stable than that corresponding to the oxidation of the hydrogenated silicon atom. However, the difference in stability is only 0.9 kcal/mol, much lower than that for the $-CH_2CH_3$ monolayer. This correlates with the fact that the repulsion among the $-$CCH groups is lower than among the $-CH_2CH_3$ groups.

An investigation using scanning auger microscopy indicated that the alkylated surfaces formed oxide in isolated, inhomogeneous patches on the surface.[24] Hence, lateral oxide growth and propagation is inhibited by even a partial coverage of Si$-$C bonds. The inhibition of lateral oxide growth can be understood under the light of our results. On a partially covered surface, lateral oxide growth implies the successive oxidation of hydrogenated and alkylated silicon atoms. However, the oxidation of the backbonds of alkylated silicon atoms is more stable than the oxidation of the backbonds of hydrogenated silicon atoms. As discussed before, this energy difference is 5.4 kcal/mol for a methyl monolayer and 10.4 kcal/mol for an ethyl monolayer. Therefore, the lateral oxidation of alternating alkylated and hydrogenated silicon atoms has an energetic corrugation which increases with the chain length. We therefore attribute the formation of the experimentally observed oxide patches to the presence of this energetic corrugation. In the case of the hydrogenated Si(111) surface, oxide growth also occurs via homogeneous nucleation of small two-dimensional oxide clusters in the topmost bilayer, which are randomly distributed over the flat terraces.[52] This implies that on this ungrafted surface the energy barriers for lateral oxide growth are also high. We think that these barriers should increase on the grafted surfaces, although this requires the calculation of activation energy barriers for confirmation.

Conclusions

Periodic density functional calculations and local MP2 calculations on cluster models of the surface were employed to study the influence of intermolecular interactions and subsurface oxidation on the structure and stability of compact monolayers of small organic and inorganic molecules bound to the Si(111). We considered the following modified surfaces: Si$-CH_3$, Si$-$CCH, Si$-$CN, Si$-CH_2CH_3$, Si$-OCH_3$, Si$-$OH, Si$-NH_2$, Si$-$NHOH, and Si$-ONH_2$.

Although the intermolecular separation of 3.84 Å in the (1 $\times$ 1) compact structures is smaller than the van der Walls diameter of most of the molecules, LMP2 calculations show that the intermolecular repulsion is relatively small for all the molecules investigated. This explains the fact that for ethyl monolayers, coverages around 80% have been reported with different experimental techniques.[8,24] In the case of the $-$NHOH terminated silicon surface, an attractive interaction of 7.5 kcal/mol was observed as a consequence of the formation of OH$\cdots$N and NH$\cdots$O hydrogen bonds.

Subsurface oxidation was investigated for $-$H, $-CH_3$, and $-CH_2CH_3$ terminated surfaces with surface coverages of 100 and 50%. The oxidation of the third Si$-$Si backbond is considerably more exothermic than the oxidation of the first and second backbonds. For a surface coverage of 50%, we found that the structures which have the backbonds of the alkylated silicon atom oxidized are more stable than the structures in which the hydrogenated silicon atom is oxidized. This introduces an important corrugation in the potential energy surface. The oxidation of alkylated silicon atoms stabilizes the organic monolayer for two reasons: a decrease of repulsive interactions between adjacent alkyl chains and a strengthening of the Si$-$C surface bond.

Subsurface oxidation increases the strength of the Si$-$C bond by 18.4 kcal/mol. This correlates with thermal stability studies which find that the Si$-$C bond remains intact on the oxidized silicon surfaces[51] whereas it cleaves on the unoxidized surface.[49,50]

Activation energy barriers for the hydroxylation reaction with water were calculated to evaluate the reactivity of the different grafted surfaces. The energy barriers for the alkylated surfaces (ca. 40 kcal/mol) are considerably higher than for the hydrogenated surface (28.4 kcal/mol). Introduction of conjugation in the organic molecule decreases the activation energy barrier. The bonding of electronegative atoms to the surface favors the nucleophilic attack of water to the silicon atom. The lowest activation barriers were obtained for the $-NH_2$ (7.9 kcal/mol) and $-$Cl (13.4 kcal/mol) terminated surfaces. The small activation barrier for the chlorinated surface correlates with the high reactivity of this surface toward oxidation.[24] The nucleophilic attack of water is also facilited by subsurface oxidation. The activation barrier for the hydroxylation of the Si$-CH_3$ surface decreases from 40.3 kcal/mol on the unoxidized surface to 31.2 kcal/mol on the oxidized surface.

Acknowledgment. Financial support from FONCyT (Grant PICT 2005-32893), CONICET (Grant PIP 5903), and SECYT-UNC is gratefully acknowledged. M.F.J. and F.A.S. thank CONICET for the fellowships granted.

References and Notes

(1) Leftwich, T. R.; Teplyakov, A. V. *Surf. Sci. Rep.* **2008**, *63*, 1.
(2) Buriak, J. M. *Chem. Rev.* **2002**, *102*, 1271.
(3) Boukherroub, R. *Curr. Opin. Solid State Mater. Sci.* **2005**, *9*, 66.
(4) Sieval, A. B.; van der Hout, B.; Zuilhof, H.; Sudholter, E. J. R. *Langmuir* **2000**, *16*, 2987.
(5) Sieval, A. B.; van der Hout, B.; Zuilhof, H.; Sudholter, E. J. R. *Langmuir* **2001**, *17*, 2172.
(6) Wallart, X.; Henry de Villeneuve, C.; Allongue, P. *J. Am. Chem. Soc.* **2005**, *127*, 7871.
(7) Linford, M. R.; Chidsey, C. E. D. *J. Am. Chem. Soc.* **1993**, *115*, 12631.
(8) Webb, L. J.; Rivillon, S.; Michalak, D. J.; Chabal, Y. J.; Lewis, N. S. *J. Phys. Chem. B* **2006**, *110*, 7349.
(9) Webb, L. J.; Nemanick, E. J.; Biteen, J. S.; Knapp, D. W.; Michalak, D. J.; Traub, M. C.; Chan, A. S. Y.; Brunschwig, B. S.; Lewis, N. S. *J. Chem. Phys. B* **2005**, *109*, 3930.
(10) Fidélis, A.; Ozanam, F.; Chazalviel, J. -N. *Surf. Sci.* **2000**, *444*, L7.
(11) Yu, H.; Webb, L. J.; Ries, R. S.; Solares, S. D.; Goddard, W. A.; Heath, J. R.; Lewis, N. S. *J. Phys. Chem. B* **2005**, *109*, 671.
(12) Hurley, P. T.; Nemanick, E. J.; Brunschwig, B. S.; Lewis, N. S. *J. Am. Chem. Soc.* **2006**, *128*, 9990.
(13) Rohde, R. D.; Agnew, H. D.; Yeo, W.-S.; Bailey, R. C.; Heath, J. R. *J. Am. Chem. Soc.* **2006**, *128*, 9518.

(14) Nemanick, E. J.; Hurley, P. T.; Brunschwig, B. S.; Lewis, N. S. *J. Phys. Chem. B* **2006**, *110*, 14800.
(15) Faucheux, A.; Gouget-Laemmel, A. C.; Henry de Villeneuve, C.; Boukherroub, R.; Ozanam, F.; Allongue, P.; Chazalviel, J.-N. *Langmuir* **2006**, *22*, 153.
(16) Gorostiza, P.; Henry de Villeneuve, C.; Sun, Q. Y.; Sanz, F.; Wallart, X.; Boukherroub, R.; Allongue, P. J. *Phys. Chem. B.* **2006**, *110*, 5576.
(17) Zhang, X.; Chabal, Y. J.; Christman, S. B.; Chaban, E. E.; Garfunkel, E. *J. Vac. Sci. Technol., A* **2001**, *19*, 1725.
(18) Tachibana, A.; Sakata, K.; Sato, T. *Jpn. J. Appl. Phys.* **1998**, *37*, 4493.
(19) Ogawa, H.; Ishikawa, K.; Inomata, C.; Fujimura, S. *J. Appl. Phys.* **1996**, *79*, 472.
(20) Yasaka, T.; Takakura, M.; Sawara, K.; Uenaga, S.; Yasutake, H.; Miyazaki, S.; Hirose, M. *IEICE Trans. Electron.* **1992**, *E75-C*, 764.
(21) Miura, T.; Niwano, M.; Shoji, D.; Miyamoto, N. *J. Appl. Phys.* **1996**, *79*, 4373.
(22) Niwano, M.; Kageyama, J.; Kurita, K.; Kinashi, K.; Takahashi, I.; Miyamoto, N. *J. Appl. Phys.* **1994**, *76*, 2157.
(23) Ikeda, H.; Hotta, K.; Yamada, T.; Zaima, S.; Iwano, H.; Yasuda, Y. *J. Appl. Phys.* **1995**, *77*, 5125.
(24) Webb, L. J.; Michalak, D. J.; Biteen, J. S.; Brunschwig, B. S.; Chan, A. S. Y.; Knapp, D. W.; Meyer, H. M., III; Nemanick, E. J.; Traub, M. C.; Lewis, N. S. *J. Phys. Chem. B.* **2006**, *110*, 23450.
(25) Solares, S. D.; Yu, H.; Webb, L. J.; Lewis, N. S.; Heath, J. R.; Goddard, W. A., III. *J. Am. Chem. Soc.* **2006**, *128*, 3850.
(26) Solares, S. D.; Michalak, D. J.; Goddard, W. A., III; Lewis, N. S. *J. Phys. Chem. B* **2006**, *110*, 8171.
(27) Nemanick, E. J.; Solares, S. D.; Goddard III, W. A.; Lewis, N. S. *J. Phys. Chem. B* **2006**, *110*, 14842.
(28) Halls, M. D.; Raghavachari, K. *J. Phys. Chem. B* **2004**, *108*, 19388.
(29) Jones, G.; Jenkins, S. J.; King, D. A. *Surf. Sci.* **2006**, *600*, L224.
(30) Carot, M. L.; Macagno, V. A.; Paredes-Olivera, P.; Patrito, E. M. *J. Phys. Chem. C* **2007**, *111*, 4294.
(31) Baroni, S.; Dal Corso, A.; De Gironcoli, S.; Giannozzi, P. http://www.pwscf.org.
(32) Vanderbilt, D. *Phys. Rev. B* **1990**, *41*, 7892.
(33) Perdew, J. P.; Burke, K.; Ernzerhof, M. *Phys. Rev. Lett.* **1996**, *77*, 3865.
(34) Monkhorst, H. J.; Pack, J. D. *Phys. Rev. B* **1976**, *13*, 5188.
(35) Møller, C.; Plesset, M. S. *Phys. Rev.* **1934**, *46*, 618.
(36) Sæbø, S.; Pulay, P. *Theor. Chim. Acta* **1986**, *69*, 357.
(37) Sæbø, S.; Pulay, P. *Annu. Rev. Phys. Chem.* **1993**, *44*, 213.
(38) Sæbø, S.; Tong, W.; Pulay, P. *J. Chem. Phys.* **1993**, *98*, 2170.
(39) Pipek, J.; Mezey, P. G. *J. Chem. Phys.* **1989**, *90*, 4916.
(40) Kendall, R. A.; Dunning, T. H.; Harrison, R. J. *J. Chem. Phys.* **1992**, *96*, 6796.
(41) *Jaguar 4.2*; Schrodinger, Inc.: Portland, OR, 2000.
(42) Michalak, D. J.; Rivillon, S.; Chabal, Y. J.; Esteve, A.; Lewis, N. S. *J. Phys. Chem. B* **2006**, *110*, 20426.
(43) Solares, S. D.; Michalak, D. J.; Goddard, W. A., III.; Lewis, N. S. *J. Phys. Chem. B* **2006**, *110*, 8171.
(44) Yu, H.; Webb, L. J.; Solares, S. D.; Cao, P.; Goddard, W. A., III.; Heath, J. R.; Lewis, N. S. *J. Phys. Chem. B.* **2006**, *110*, 23898.
(45) Sieval, A. B.; van den Hout, B.; Zuilhof, H.; Sudholter, E. J. R. *Langmuir* **2001**, *17*, 2172.
(46) Soria, F. A.; Patrito, E. M.; Paredes-Olivera, P. Unpublished work, 2008.
(47) Kanai, Y.; Takeuchi, N.; Car, R.; Selloni, A. *J. Phys. Chem. B* **2005**, *109*, 18889.
(48) Carpenter, J. E.; Weinhold, F. *J. Mol. Struct.* **1988**, *169*, 41.
(49) Faucheux, A.; Yang, F.; Allongue, P.; Henry de Villeneuve, C.; Ozanam, F.; Chazalviel, J.-N. *Appl. Phys. Lett.* **2006**, *88*, 193123.
(50) Sung, M. M.; Kluth, G. J.; Yauw, O. W.; Maboudian, R. *Langmuir* **1997**, *13*, 6164.
(51) Kluth, G. J.; Sung, M. M.; Maboudian, R. *Langmuir* **1997**, *13*, 3775.
(52) Neuwald, U.; Hessel, H. E.; Feltz, A.; Memmert, U.; Behm, R. *Appl. Phys. Lett.* **1992**, *60*, 1307.

JP711307P